INVESTIGATION OF HIGH-ENERGY NUCLEAR-ACTIVE PARTICLES AT SEA LEVEL

V. A. DMITRIEV, G. V. KULIKOV, and G. B. KHRISTIANSEN

Institute of Nuclear Physics, Moscow State University

Submitted to JETP editor January 26, 1959

J. Exptl. Theoret. Phys. (U.S.S.R.) **37**, 893-905 (October, 1959)

We consider large bursts in an ionization chamber under an absorber that is highly efficient to nuclear interactions. It is shown that at sea level most large bursts (≥ 1000 relativistic particles) are due to interactions of nuclear-active particles with energies $E \geq 10^{12}$ ev in the absorber. The spectrum of the nuclear-active particles and their air accompaniment are given. The accompaniment observed can be attributed to fluctuations in the development of the nuclear shower in the atmosphere. Conclusions are drawn concerning the cross section for the interaction between the nuclei of the atmospheric atoms and particles of energies approximately 10^{13} ev. Cases of high-energy nuclear-active particle beams have been observed.

INTRODUCTION

THE absorption coefficient, the energy spectrum, and the shower accompaniment of high energy nucleons are all connected with the elementary characteristics of nuclear collisions, and their investigation is therefore of considerable interest. Several experiments were recently performed on high mountains, in which nuclear-active particles were investigated by means of bursts in ionization chambers under various absorbers. No analogous work was performed at sea level, and the bursts observed at sea level by Carmichael et al.[1] under layers of lead of different thickness were wholly attributed to μ-meson bursts.

In this connection, we investigated large bursts and their air accompaniment with the aid of apparatus that had a high counting efficiency for nuclear-active high-energy particles. The measurements were performed during 1957 with apparatus, presently in operation at the Moscow State University, intended for an exhaustive investigation of extensive atmospheric showers.

METHOD AND DESCRIPTION OF APPARATUS

The nuclear-active (n.a.) high-energy particles were detected by the electron-nuclear (e.n.) showers that develop in dense matter.[2,3] In a dense medium almost all the energy of the n.a. particles is consumed, in the final analysis, in ionization of the medium and only a small fraction is used for rearrangement of the atomic nuclei. Therefore, by measuring the ionization simultaneously under layers of various thickness, we can determine the n.a. particle energy that gives rise to the shower.[4] However, an approximate measurement of the energy of n.a. particles of high energy ($E \geq 10^{12}$ ev) can also be performed by measuring the ionization under a layer of matter of single thickness, by using an absorber made up of two different substances — a thick layer of a low-Z substance and a thin layer of a high-Z one. (Such an absorber was used earlier.[5]) If the thickness of the low-Z amounts to several nuclear ranges, then a considerable fraction of the energy of the n.a. particles will be converted in it into an electron-photon (e.p.) component; this fraction will change little from

case to case. In the low-Z layer the e.p. cas-
cades due to π^0 mesons will be only weakly de-
veloped, since such a layer corresponds to a
small number of t -units. In the high -Z layer
the electron-photon cascades will develop further
and will soon reach a maximum. The number of
particles in the cascade maximum is proportional
to the energy of the electron-photon component
incident on the layer. The depth at which the max-
imum is reached depends only logarithmically on
the initial energy of the photons and electrons,
and remains practically constant at large ener-
gies. All this makes it possible to measure the
energy of high-energy nuclear-active particles
incident on such an absorber, by using only a
single array of ionization chambers.

We used four ionization chambers, with a total
effective area of 1 m². A total of 720 Geiger-
Müller counters* were used to register the charged-
particle currents accompanying the nuclear-active
particle showers. This permitted us to determine
the thickness of the air accompaniment over a wide
range and with a much greater accuracy than pre-
viously obtained.[1,6,7] Furthermore, in some ex-
periments we located 48 counters beneath the cham-
bers and inserted 10 centimeters of iron between
the counters and the chambers. The arrangement
and a section through the nuclear-active particle
detector is shown in Fig. 1 of reference 10. The
absorber of the nuclear-active particle detector
consists of several layers: a layer of lead† 5 cm
thick, a layer of graphite (specific gravity 1.68
g/cm³) 70 cm thick, and a layer of lead 2 cm
thick. The first two layers make up approximately
1.8 of the range of nuclear interaction in matter
(assuming that the ranges of 160 g/cm² for lead
and 70 g/cm² for graphite, obtained at lower ener-
gies, also hold for the energies under considera-
tion here). The detector therefore has high effi-
ciency for nuclear interactions.

It was necessary to cover the graphite from
above with lead to reduce the penetration of the
electron-photon component of extensive atmos-
pheric showers (e.a.s.) capable of producing large
bursts under the graphite layer and in the lower
lead layer. The presence of a thick layer of lead
greatly softened the energy spectrum of the soft
component of the e.a.s. before it entered the
graphite, and led to an almost complete screening
of the chambers from the soft component of the
e.a.s. The apparatus was controlled by pulses

*For a detailed description of the arrangement and the ap-
paratus see references 8–10.

†In the case of nuclear-active particles accompanied by a
shower with N $\geq 10^5$, the data used have been obtained with a
detector in which the upper lead layer has been increased to
8 cm.

from the chambers whenever the amplitudes of
the latter exceeded a specified value. The rise
time of the chamber pulses was 30 μsec, and
therefore the delay in operation of the threshold
circuit that segregated the pulses by amplitudes,
at pulse amplitudes close to threshold, was not
less than 30 microseconds. However, the resolv-
ing time of the hodoscope setup was 10 − 12 μsec.
The hodoscope was therefore controlled by two
circuits, one with a threshold one-tenth that of
the other. The pulse rise in the cylindrical cham-
ber was close to linear for nonlocal ionization,[11]
and therefore the delay in operation of the first
circuit was considerably less. The pulse from
the first circuit controlled the hodoscope and the
amplitude analyzer, but the data were recorded
only when the second threshold circuit was trig-
gered. This insured coordinated operation of the
chambers and hodoscopes. The threshold value of
the pulse from the chamber needed to operate both
circuits corresponded to the passage of 800 relati-
vistic particles along the central chord of the cham-
ber. The nuclear-active particles that produced in
the absorber a shower of 1000 particles or more
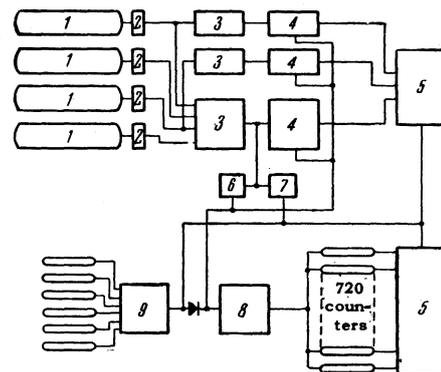were registered with a probability of 100%.

FIG. 1. Block diagram showing connection of chambers
and counters. 1 − ionization chambers, 2 − preamplifiers,
3 − amplifiers, 4 − amplitude analyzers, 5 − counting devices,
6 and 7 − threshold circuits, 8 − hodoscope GK-7, 9 − six-fold
coincidence circuit.

A block diagram of the apparatus is shown in
Fig. 1. The entire apparatus was placed in a spe-
cial room with a roof made of duraluminum and
foamed plastic. The total amount of matter over
the apparatus was not less than 2.0 g/cm².

RESULTS

During the operating time of the setup (~ 1300
hours) we registered a total of 948 bursts, each
corresponding to the passage of 1000 and more
relativistic particles along the central chord of
the chamber. The mean frequency of the bursts
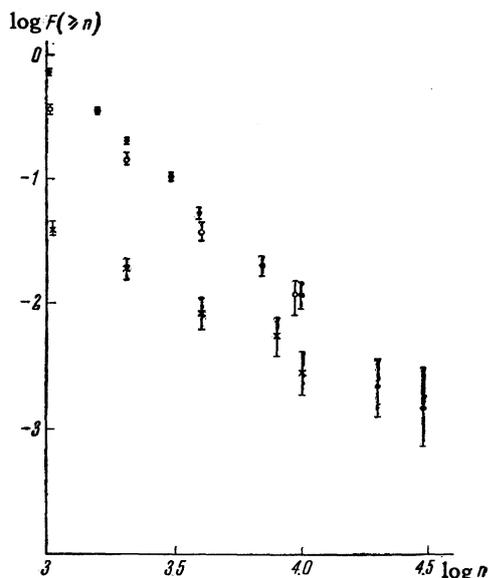at n ≥ 1000 was found to be (0.70 ± 0.04)

FIG. 2. Spectrum of bursts in chambers at $n \geqslant 1000$ relativistic particles. Abscissas — logarithm of burst measured in "average" relativistic particles; ordinates — logarithm of number of bursts greater than n/hr-m²; ● — total number of bursts; ○ — burst spectrum at aerial accompaniment of $N \geqslant 3 \times 10^2$; × — spectrum of bursts in chambers at a shower accompaniment with $N \geqslant 10^4$.

$hr^{-1}m^{-2}$. The burst spectrum is shown in Fig. 2. The observed bursts could be caused by: 1) the soft component of extensive atmospheric showers, 2) radiation bursts from high-energy muons, 3) strongly ionizing products of nuclear disintegrations of low energy, and finally, 4) nuclear interactions in the absorber between high energy-particles that initiate electron-photon showers.

To verify the role of the bursts due to the soft component of extensive atmospheric showers, we performed preliminary experiments on the determination of the number of bursts with $n \geq 1000$

particles at various thicknesses of the upper layer of lead (2, 4, and 5 cm). With a homogeneous lead absorber, the number of large bursts due the soft component of the e.a.s. begins to diminish at absorber thickness greater than 2 cm.[1] If a layered absorber is used, the burst frequencies at 2 cm of lead differ from those of 4 cm of lead, at a threshold $n \geq 1000$, by a factor of 2.3. At 4 and 5 cm, the burst frequencies become the same (accurate to 10%). This shows that, for the particular filter employed, the role of bursts due to the soft component of e.a.s. is small.

To determine the role of the bursts connected with muons and nuclear disintegrations, we measured bursts with the same apparatus, but without placing a composite absorber over the chamber. The lead shields on the sides and bottoms of the chambers were retained. In this case we registered bursts caused by: 1) e.a.s., 2) nuclear disintegrations, 3) muons traveling at small angles to the horizontal plane. The corresponding experimental data are listed in Table I. Knowledge of the magnitudes of the bursts in the individual chambers, of the number of counters operated under the chambers, and of the number of open counters operated allows us to segregate the bursts due to various processes. (Naturally, such a segregation of bursts is not unique in individual cases, but in each group of Table I the principal part of the bursts is due only to one process.)

From the number of bursts produced by muons traveling at small angles to the horizontal surface we can determine the total number of bursts caused by muons in the composite absorber. Actually, the angular distribution of the muons can be readily obtained by assuming the cosmic radiation to be isotropic, by assuming the pions and the muons to stay

TABLE I. Bursts in chambers without filter above

	Classification of events	Number of events	Number of bursts per hr-m²
I	Bursts in all chambers, accompanied by a nuclear-active shower (minimum number of counters operating in these cases under the chamber is 10).	9	0.07
II	Bursts in one chamber; less than 6 counters operated under the chamber (bursts due to stars in the chamber walls and in the argon)	17	0.13
III	Bursts in three and four chambers. Less than 5 counters operated under the chamber (bursts due to muons traveling at larger angles with the vertical)	10	0.08
IV	Other cases: a) bursts in one chamber; 10 (13) counters operated under the chamber b) bursts in three chambers; 9 counters operated under the chamber (Aerial accompaniment in these cases amounted to 5—10 counters)	2 1	0.02

TABLE II. Distribution of large bursts by number of counters
operated under the chambers at various air accompaniments

Number of counters operated under the chambers	Number of aerial-accompaniment counters operated								
	0	1—2	3—4	5—9	10—29	≥30	medium shower N ~ 10^4	large shower N ~ 10^5	total number of cases
0	11	3							14
1—2	8	2						1	11
3—4	3	4							7
5—9	3	2							5
10—24	7	8	2	3	7	1	2	3	33
≥25	1	5	2	3	2	5	4	4	26
Total number of cases	33	24	4	6	9	6	6	8	96

in the direction of the primary particles, and by
assuming that the pion-absorption range equals
the interaction range.* At sea level, the number
of muons with energies E, E +dE, traveling at
an angle θ is

$$J^\mu (E,\theta) = CA (E)/[1 + (L(E)/Z_0) \cos \theta] ,$$

where L(E) is the decay range of pions with en-
ergy E, $Z_0 = x/\rho$ is a constant relating depth and
pressure in the atmosphere, A(E) is the number
of pions of energy E along the vertical, and C is
a constant.

In calculating the number of bursts we took into
account the geometry of our setup and the reduction
in effective muon energy with increasing path of par-
ticles of the radiation shower in the chambers; the
spectrum of the muons was assumed to obey a power
law with exponent[13] $\gamma = - 2.5$. Assuming that the
number of mesons passing through the side walls
of the absorber and causing bursts with n ≥ 1000
is approximately 0.1 $hr^{-1}m^{-2}$, we obtain approxi-
mately 0.2 $hr^{-1}m^{-2}$ for the total number of bursts
due to muons in the absorber.

Thus, the bulk of the bursts at sea level, under
the absorber used, is due to high-energy nuclear-
active particles.†

The presence of hodoscopic counters under the
chamber during the time of some of the principal
measurements also made it possible to segregate,
in individual cases, the bursts due to different
processes. Data on the accompaniment of large
bursts (n ≥ 1000) with operation of counters
under the chambers and air accompaniment of
the bursts are listed in Table II.

As can be seen from Table II, the fraction of
bursts accompanied by operation of a small num-

---

*Assumptions usually made in calculating the altitude
variation of muons (see, for example, reference 12).

†It follows from the data of reference 14 that the number of
bursts due to nuclear-active particles of high energy decreases
slowly at absorber thicknesses up to 50 cm lead, and more
rapidly at 50–80 cm lead. It is therefore erroneous to attribute,
as is done in reference 1, a muon origin to large bursts, whose
number decreases slowly up to 27 cm lead.

ber (≤ 5) of counters under the chamber amounts
to $\frac{1}{3}$, in agreement with the data of the control
experiment (groups I and III of Table I). We note
that the data given in Tables I and II exaggerate
the role of nuclear disintegrations, since the area
of the counters under the chambers equals the area
of the chambers, and the distance between cham-
bers is of the order of their linear dimensions. In
the case of passage of an electron-photon cascade
through the edge of the region occupied by the
counters, the number of operated counters de-
creases and such a case can be classified as a
nuclear disintegration.

It is seen also from Table II that among the 40
cases with air accompaniment, equivalent to the
operation of three or more counters, only in one
case did less than ten counters operate under the
chamber. This permits us to state that the role
of nuclear disintegration is small in this group.
The required presence of air accompaniment al-
lows us to state that the role of bursts due to
muons in this group is also small. The bulk of
the bursts with such air accompaniment is thus
due to high-energy nuclear interactions in the ab-
sorber. The spectrum of bursts of this group
(Fig. 2) can be represented by a power law with
exponent equal to $\gamma = - 1.5 \pm 0.2$. The number of
bursts with n ≥ 1000 without air accompaniment,
which (as already indicated[9]) is due to a consid-
erable part to nuclear disintegrations, diminishes
more steeply (exponentially). From data of other
investigations, the spectra of bursts due to muons
and strongly-ionizing products of nuclear disinte-
grations are also characterized by a steep drop.[1,13]
The spectrum of bursts due to muons, according to
the data of the control experiment, also has a steep
drop, corresponding to a power law with exponent
$\gamma \simeq - 2.6$ (the number of such cases is small).
The total burst spectrum (Fig. 2) is character-
ized by an exponent $\gamma = - 1.7 \pm 0.15$. This indi-
cates that the role of nuclear-active particles be-
comes predominant in the region of large bursts.
If we consider the region of bursts with n ≥ 5000

TABLE III. Lateral structure of bursts under differing air
accompaniment (bursts in 2 non-adjacent chambers,
the smaller comprising a fraction x of the total)

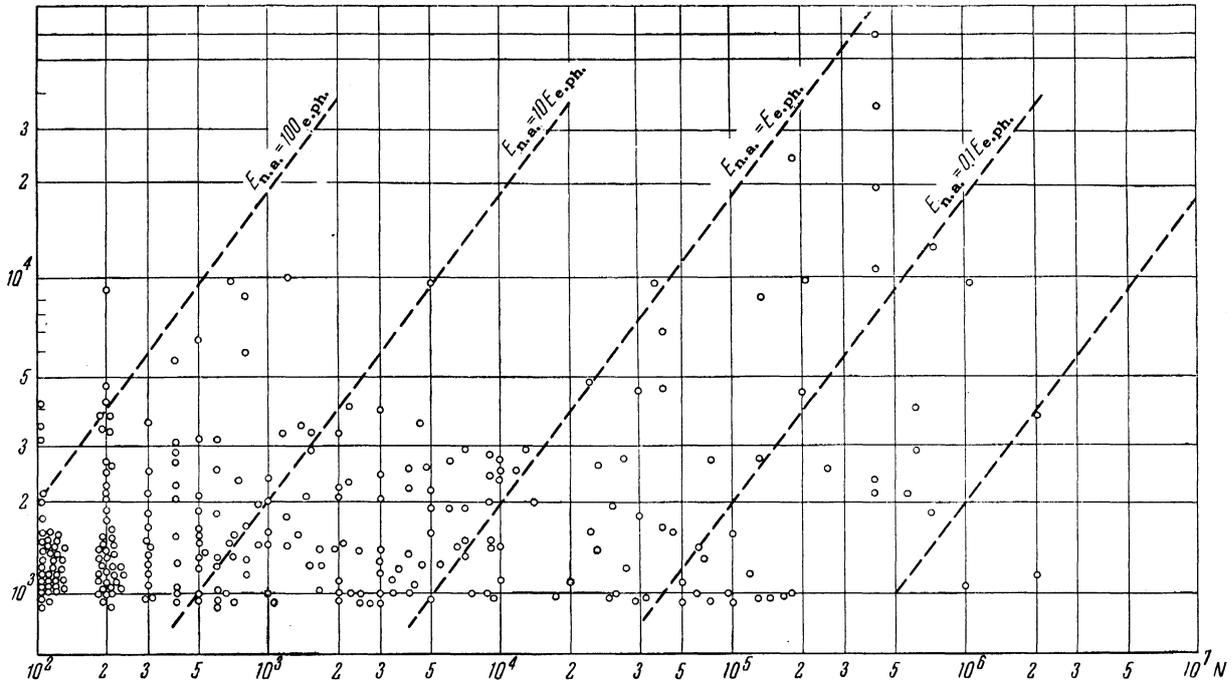| x	Air accompaniment			x	Air accompaniment		
	0—4	5	showers $N \geqslant 1 \cdot 10^4$		0—4	5	showers $N \geqslant 1 \cdot 10^4$
~1	3	0	4	$\geqslant 0.01$	5	8	9
$\geqslant 0.1$	7	7	11	< 0.01	64	36	6

FIG. 3. Magnitude and accompaniment distribution vs. number of particles N in air shower; ordinate — burst measured in "average" relativistic particles, n.

and assume that the spectrum of bursts due to muons and disintegrations is characterized by an exponent $\gamma = -2.5$, the role of such bursts decreases to approximately 10%.

In some cases the burst results from two or more high-energy nuclear-active particles striking the apparatus. Such are cases of large bursts in two non-adjacent chambers and cases of extensive bursts, giving commensurate (differing by a factor of less than 5) bursts in three chambers. The latter cannot be explained by the broad angular distribution of the electrons emitted from the lead.*

Table III gives data pertaining to the structure of the bursts. A fraction of the extensive bursts (one column of the table) is caused by high-energy muons.

The processing of hodoscopic data of a portion of the experiments makes it possible to determine the thickness of the air accompaniment of nuclear-active particles. Figure 3 represents a distribution of the part of the bursts in magnitude and thickness of air accompaniment. Figure 4 shows the
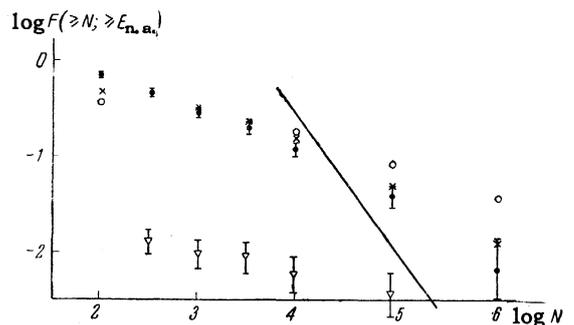

FIG. 4. Nuclear-active particle distribution vs. number of particles N in the accompaniment; ● — bursts with $n \geqslant 1000$, ∇ — with $n \geqslant 10,000$ relativistic particles. Ordinate — logarithm of the number of nuclear active particles per hr-m², accompanied by a shower with more than N particles. o, x — calculated data, each event results in: o — 7 particles of energy 0.1 E or x — 1 particle of 0.3 E, one particle of 0.2 E, and 1 particle of 0.1 E. Solid curve — shower spectrum.

*We calculated the magnitude of the burst in the chamber assuming isotropic distribution of the particles in the shower under the lead, obviously the limiting case. It was found that even under this assumption the burst in the third chamber was 8% smaller than the summary one, while in the neighboring chamber the burst amounted to 22% of the summary one with the shower axis located at the center of the first chamber.

distribution relative to the number of particles in the shower, accompanying the nuclear-active particles causing a burst with $n \geq 1000$ and with $n \geq 10,000$. The spectrum of the bursts of accompaniment by an e.a.s. with $N \geq 1 \times 10^4$ is also shown in Fig. 2. The spectrum can be described by a power law with exponent $\gamma = -1.0 \pm 0.2$.

DISCUSSION OF RESULTS

As already noted, the magnitude of the burst in the ionization chamber located under an absorber is proportional to the energy transferred to the π^0 mesons during nuclear interactions of high-energy particles in the absorber. The value of the coefficient k' of proportionality between the energy of the primary particle and the mean magnitude of the burst n, expressed in relativistic particles, was derived previously for a given energy of primary particle.[10] However, one must take into account the spread in the energy transferred, caused by various possible interactions in the absorber between the primary particle and the particles of successive generations, even in a non-fluctuating event, but in the case of a steeply descending primary-particle energy spectrum. The value of the coefficient k of proportionality between the magnitude of the burst and the mean energy of the particle causing the burst of fixed magnitude in the chamber will therefore differ from k'. To estimate the resultant variation of the coefficient, we have calculated the coefficient k under the following assumptions: a) the incident particle is a nucleon, b) the interaction range of high-energy particles in graphite is independent of the particle energy and equals[15] 70 g/cm^2, c) the fraction of the energy transferred to the mesons in each event is independent of the nucleon energy E_0 and equals $0.4 E_0$, and $\frac{1}{3}$ of the initial pion energy is transferred to the π^0 mesons, d) the principal faction of the energy ($\sim$1) transferred in the interactions to the $\pi^{\pm}$ mesons is carried by one meson.

We determine the energy transferred by the first three generations of the nuclear cascade developed in graphite to the electron-photon component, for a given number of interactions between the particles of these generations. In finding the mean energy transferred at a fixed burst magnitude, the energy spectrum of the nuclear-active particles incident on the apparatus was assumed to obey a power law with exponent $\gamma = -1.5$. The development of electron-photon showers in lead was considered on the basis of the data of reference 16. The spectra of the secondary π^0 mesons were not known, and we therefore chose the mean number of particles under lead obtained under the assumption that the shower

was due to one γ quantum with energy E_γ, or to the number of γ quanta of equal energy, as expected from the Landau theory (it was assumed that the number of γ quanta equals twice the effective number of mesons[17]). The value thus obtained for the coefficient necessary to convert the number of particles in the burst to the energy of the particle causing the burst, is $k = 8 \times 10^8$ ev for a particle energy 1×10^{12} ev. At higher particle energies, the electron-photon cascades do not reach maximum development in the lower layer of lead, causing an increase in the coefficient k with energy. However, the energy of the π^0 mesons generated by the secondary $\pi^{\pm}$ mesons is considerably less than the energy of the π^0 mesons generated by nucleons, and the fraction of the energy carried by the π^0 mesons is considerable. This reduces the dependence of k on the energy.

For particle energies $E_0 = 4 \times 10^{12}$ ev we obtain, with allowance for the foregoing circumstance, $k = 1 \times 10^9$ ev whereas for $E_0 = 4 \times 10^{13}$ ev we get $k = 1.4 \times 10^9$ ev. Data on bursts caused by nuclear-active particles pertain therefore to the 10^{12}–4×10^{13} ev energy domain.

1) <u>Interaction of nuclear-active particles of high energy in the atmosphere.</u> The results obtained yield data on the character of the nuclear interactions that determine the passage of high-energy nuclear-active particles through the atmosphere.

As already noted, large bursts with $n \geq 5000$ relativistic particles are caused by showers from nuclear-active particles. One can therefore compare our data on the intensities of such bursts with the data pertaining to the level of Pamir (652 g/cm^2),[14] where the relative role of the bursts due to muons is generally small. The apparatus used in reference 14 was similar to ours, the chamber dimensions were almost the same, and the pressure in the chambers was the same. This makes possible a direct comparison of the data obtained with the two setups. It must be taken into account in the comparison that when a composite filter with graphite is used the number of bursts is greater by a factor of approximately 2 than when a solid lead absorber is used.[5] Equipment similar to ours registers the nuclear-active particles within a large angle; assuming therefore that we register the global intensity at both altitudes, we obtain for the connection between the frequency of the bursts, registered at the Moscow level (C_M) and at the Pamir level (C_P) the following expression (see, for example, reference 17):

$$C_M / C_P = 2 [(\mu x_{\bar{P}} + 1)/(\mu x_M + 1)] \exp\{-\mu(x_M - x_P)\},$$

where x_M is the Moscow depth and x_P the Pamir

depth. The absorption range of nuclear-active particles with energies $E \geq 5 \times 10^{12}$ ev, determined from these data, is found to be $\lambda_{abs} = 1/\mu = (124 \pm 14) \text{ g/cm}^2$.

The data available[2,18,19] on the intensity of the primary component also make it possible to determine the value of the range for the absorption of nuclear-active particles with energies $E \geq 5 \times 10^{12}$ ev. Averaging the intensities given by Elliott[18] and Cocconi,[19] we obtain $\lambda_{abs} = (120 \pm 6) \text{ g/cm}^2$ (the errors are determined by the extreme values of the intensity of the primary component as given in these papers and by the statistical accuracy of our own measurements).

The data represented in Fig. 2 can be recalculated for the domain of larger bursts n > 5000, with allowance for the energy dependence of the coefficient k. The graph obtained is shown in Fig. 5 and represents the energy spectrum of nuclear-active particles in the energy range from 5×10^{12} to 5×10^{13} ev. The spectrum can be approximated by a power law with exponent $\gamma = -1.5^{+0.2}_{-0.3}$. The spectrum of nuclear-active particles of lower energies is actually shown in Fig. 2, since at lower energies the coefficient k remains practically constant. The value of the exponent in this case is $\gamma = -1.5 \pm 0.2$. The spectrum of the primary cosmic radiation in the range of energies $E \sim 10^{12}$ ev can also be approximated by a power law with exponent $\gamma = -1.5 \pm 0.1$ (reference 19). Thus, over a broad interval of nuclear-active particle energies, $10^{12} - 5 \times 10^{13}$ ev, the exponent of the energy spectrum at sea level coincides with the exponent of the primary spectrum.

The results obtained indicate that the absorption of the nuclear-active component in the atmosphere is described by a pure exponential curve, i.e., the coefficient of absorption is independent of either the depth of the atmosphere or the particle energy, at least up to $E \simeq 3$ to 5×10^{13} ev, and the exponent of the energy spectrum does not change with depth in the atmosphere.

The fact that λ_{abs} is constant outside of the dependence on the depth in the atmosphere when the exponent γ of the energy spectrum is constant is evidence that the mean characteristics of the elementary act remain unchanged up to energies exceeding, at least by a factor of several times, the energies of the particles registered at sea level (since particles with a given energy at sea level occurred in nuclear collisions of higher-energy particles).

A measurement of the fraction of cases in which the high-energy nuclear-active particle cause a burst not accompanied by a shower in air, as noted
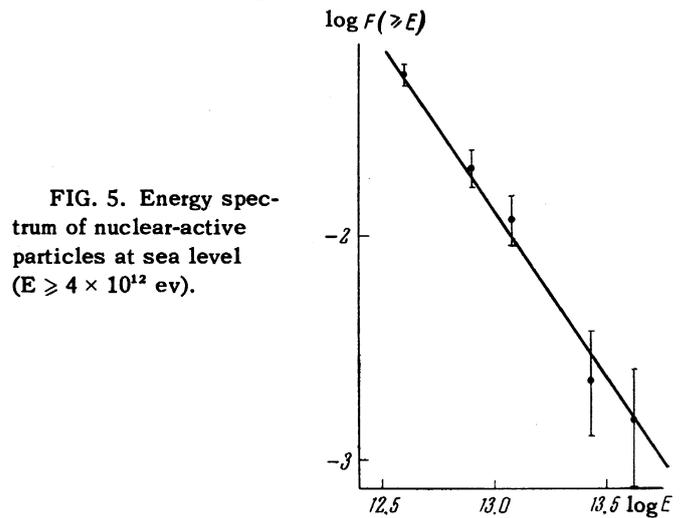

FIG. 5. Energy spectrum of nuclear-active particles at sea level ($E \geq 4 \times 10^{12}$ ev).

in reference 6, makes it possible to determine the effective cross section for inelastic collision between nucleons and the atomic nuclei of air, provided the coefficient of absorption of nuclear-active particles in the atmosphere is known.* Actually the total number M of the registered bursts, caused by a nuclear-active particle with an energy greater than a given value, is connected with the number of bursts M_0, due to particles of the same energy which experience not a single collision in the atmosphere, by the following (average) relation

$$M_0 / M = [(\mu'_{abs}x + 1)/(\mu_{int}x + 1)] \, p \exp \{- x (\mu_{int} - \mu_{abs})\},$$

where x is the depth of the point of observation, p the fraction of protons among the primary nuclei, $\lambda_{abs} = 1/\mu_{abs}$ is the range for absorption of nuclear-active particles in the atmosphere, $\lambda_{int} = 1/\mu_{int}$ is the same for the interaction of nuclear-active particles in the atmosphere (assuming that, owing to the great depth of observation, all the nuclei have experienced interactions in the atmosphere). When chambers of large area are used, it is necessary to take into account the possible simultaneous entry of two or several particles of lesser energies, contained in the shower, into the chamber. This increases the total number of bursts M of a given magnitude. An exact determination of the correction for this correlation effect can be obtained from experiments with smaller chambers. An approximate allowance for this factor can be made by introducing a coefficient p_k smaller than unity.

We note that in our setup the area of the counters registering the air accompaniment of the nuclear-active particles was 10.8 m². This made it possible to register reliably an accompaniment containing merely several hundred particles. On the other hand, the lead of the absorber in the

*The authors thank G. P. Zatsepin for valuable remarks made in discussing this and other questions.

setup was covered by a layer of low-Z substance (duraluminum, 1 cm) preventing the entrance of scattered particles of electron-photon cascades from the absorber into the counters that registered the air accompaniment of the nuclear-active particles. However, the apparatus did not make it possible, in individual cases, to distinguish bursts caused by muons from bursts caused by interactions of high-energy nuclear-active particles. The role of bursts due to muons diminishes with increasing magnitude of the bursts. Thus, the number of bursts without air accompaniment, which we observed, was due principally to higher-energy particles that experienced no interaction in the atmosphere, and to a small amount to radiation bursts caused by muons. For high-energy particles (large bursts with $n \geq 5000$) this circumstance necessitates a supplementary small term Δ in the foregoing expression

$$M_0 / M = P \exp \{-x (\mu_{int} - \mu_{abs})\} + \Delta,$$

$$\Delta = \delta(\theta) M_\mu / M, \quad P = pp_k;$$

$\delta(\theta)$ is the fraction of muons within a specified angle θ, and M_μ is the number of bursts due to muons. The value of M_μ can be obtained from control-experiment data. The magnitude of $\delta(\theta)$ can be estimated, for mesons of fixed energy, from the formulas given above for the angular distribution of the mesons.

If the number of registered bursts is small, the foregoing formula, which is correct for medium magnitudes, cannot be used. It is necessary to use the expression for the probability of experimentally observing m bursts without air accompaniment from among the observed n bursts, as a function of λ_{int}. Using the Bayes theorem we obtain the distribution for the probability λ_{int} in this case

$$W(\lambda_{int}) = C [P \exp \{-x (\mu_{int} - \mu_{abs})\} + \Delta]^m$$

$$\times [1 - P \exp \{-x (\mu_{int} - \mu_{abs})\}]^{n-m},$$

where C is a constant.

We registered 26 bursts with $n \geq 5000$, of which only one was not accompanied by a shower. This burst was due to ionization in one chamber only and was accompanied by operation of 9 counters under the chambers. Taking the geometry of the setup into account, we calculated the value of $\delta(\theta)$ for mesons capable of producing bursts with $n \geq 5000$. Figure 6 shows a plot of $W(\lambda_{int})$ for $n \geq 5000$, plotted under the following assumptions: $\lambda_{abs} = 120$ g/cm^2, $p = 0.7$, and $p_k = 0.8$. The dotted curve for $W(\lambda_{int})$ is plotted under the as-

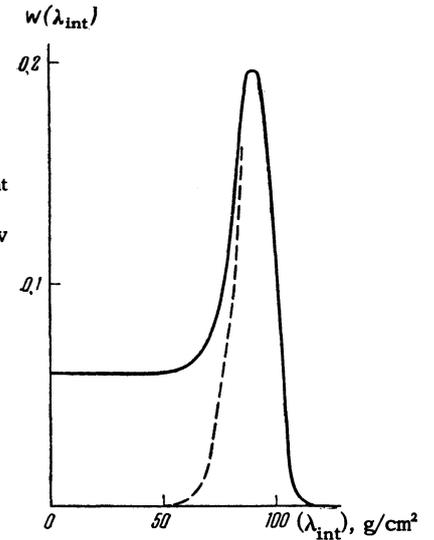FIG. 6. Probability of various values of λ_{int} for nuclear-active particles of $E \geqslant 5 \times 10^{12}$ ev (solid curve); dotted — the same under the assumption that the unaccompanied burst is due to a nucleon.

sumption the observed single burst without accompaniment is due to a nuclear-active particle. It follows from the curve that the most probable value is $\lambda_{int} = 90$ g/cm^2, and that $\lambda_{int} = 90 \pm 10$ g/cm^2 if all the bursts are caused by a nuclear-active particle. We note that the value of p_k influences the form of the curve relatively little. The obtained value of λ_{int} agrees with that recently given in other papers for considerably smaller energies $(3 \times 10^{10}$ ev). An analogous value of λ_{int} is also obtained for particles with $E \geq 10^{13}$ ev. We did not register a single particle of this energy without air accompaniment. This makes it possible to state that when $E \geq 10^{13}$ ev, $\lambda_{int} \leq 90$ g/cm^2 with a probability ~ 0.73. Thus, it can be said that the interaction cross section does not decrease at least up to $E \gtrsim 10^{13}$ ev, and that it remains constant up to $E \simeq 5 \times 10^{12}$ ev.

From the observed simultaneous incidence of several particles with $E \gtrsim 10^{12}$ ev on the chamber (see Table III) we can estimate the lateral momentum acquired by a nuclear-active particle in nuclear scattering or generation. It is obvious that for a specified distance between the nuclear-active particles, their effective generation altitude exceeds the nuclear free-path unit. At a range of 500 meters in air, we assume the effective altitude to be 1000 meters. For the observed cases of particles with $E \geq 10^{12}$ ev diverging by a distance ~ 0.5 m, we obtain $p_\perp \gtrsim 5 \times 10^8$ ev/c. We also registered one case where two nuclear-active particles, each with $E \sim 10^{13}$ ev, passed through two nonadjacent chambers. Considering that in this case both particles deviated from the initial direction, we obtain $p_\perp \lesssim 2 \times 10^9$ ev/c.

The accompaniment of nuclear-active particles

shown in Fig. 3 indicates that nuclear-active particles of such energy occur at different frequencies in showers with $N \geq 10^2$ to $N \geq 10^6$ particles.* The accompaniment of nuclear-active particles of a given energy by showers with different number of particles N is determined by the energy spectra of nuclear-active particles in the showers with different N. Vernov et al.[20] calculated the energy spectra of nuclear-active particles from one primary under various very simple assumptions concerning the character of the elementary act. Assuming, like Greisen,[2] that the number of particles in the shower N is proportional to the energy of the primary particle E, and assuming that the spectrum of the number of particles in the shower $\varphi(N)$ is described by a power law with exponent $\gamma = -2.4$ at $10^2 \leq N \leq 10^7$, we obtain curves for the accompaniment of particles with energies greater than a given value $F(\geq E, N)$ for the cases analyzed in reference 20 (see Fig. 4).

Comparison of the experimental data with the theoretical accompaniment curve shows that in the case of particles of given energy, the presence of a broad range of accompaniment intensities $(N \sim 10^2 - 10^6)$ is explained by the probabilistic character of the interaction and the finite number of interactions between nuclear-active particles of a nuclear shower and the nuclei of the atmosphere. The relative frequency of differing accompaniments is in sufficiently good agreement with the calculations for different characteristics of the elementary act; at the same time there is no need for making assumptions concerning the presence of two types of interaction, as mentioned in reference 6. To obtain agreement with the experimental data at sea level for different types of acts it is necessary, however, to modify somewhat the interaction cross section. In order to choose a particular model of the act in accordance with the accompaniment curve, it is necessary to have a more rigorous comparison of the air accompaniment (N) and the particle energy (E, E_0), particularly in the range of small N.

Let us note that, as can be seen from Fig. 4, the accompaniment curve of nuclear-active particles with $E \geq 10^{12}$ has the same character as that for $E \geq 10^{13}$ ev.

2) Nuclear-active component in low-density extensive atmospheric showers. The presence of an additional control system enabled us to study simultaneously the extensive atmospheric showers, regardless of whether they contained high-energy nuclear-active particles. Figure 4 shows a line

corresponding to the number of particles spectrum of the showers as observed by us. As can be seen from a comparison of the experimental data, nuclear-active particles with $E \geq 10^{12}$ ev are present in showers of low intensity, $N \sim 10^3 - 10^4$, but not in each shower. Since the energy of such nuclear-active particles is of the same order as (or greater than) the energy carried by the electron-photon component of the shower, the role of the nuclear-active component depends substantially on the presence or absence of such particles in an individual shower. This is seen from Fig. 3, which shows the energy and air accompaniment for each individual burst. This circumstance indicates substantial fluctuations in the development of low-intensity showers; the equilibrium between electron-photon and nuclear cascades in showers in which the energy of the nuclear-active component is too large does not exist at the observation level. Such cases can be explained, as indicated by the agreement with the calculation results given above, by a passage of a nuclear shower with weak development through the atmosphere.

From the data on the accompaniment of nuclear-active particles by showers we can also obtain the value of the energy carried by a nuclear-active high-energy particle $(E \geq 10^{12}$ ev and $E \geq 10^{13}$ ev) in a medium shower of different intensity. Actually, in showers with $N < 10^4$ the number of nuclear-active particles of such energies n $(\geq E, N)$ is small, i.e., n $(\geq E, N) < 1$. Then, knowing F $(\geq E, N)$ and $\varphi(N)$, we can find the number of particles with energies greater than a specified value n $(\geq E, N) = F (\geq E, N)/\varphi(N)$ in a medium shower. The form of the energy spectrum of particles in the region $10^{12} - 10^{13}$ ev was obtained by us, and we can therefore determine the energy carried by particles of such energies in the shower. However, the spectrum of low-density showers has not yet been investigated. To estimate the energy we extrapolated our shower spectrum to the region of lower N, using the same spectrum exponent, a fact that can only lead to an overestimate of the number of low-density showers, i.e., to an underestimate of the fraction of high-energy nuclear-active particles. The results on the distribution of energy carried by a high-energy nuclear-active particle are listed below.

Number of particles in the shower:	1×10^3 to 3×10^3	3×10^3 to 1×10^4
Ratio of the energy carried by a nuclear-active particle to the energy of the electron-photon component at the following nuclear-active particle energy:		
$E \geq 10^{12}$	6%	7%
$E \geq 10^{13}$	1%	1.5%

---

*Strictly speaking, a certain part of the bursts with accompaniment $N \sim 10^2$ can be due to muons.

The energy of the electron-photon component was determined by us as $E_{ep} = 3\beta\overline{N}$, where $\overline{N}$ is the average number of particles in the shower within the considered range of N, and β is the critical energy in air.

To estimate the mean value of the total energy carried by the nuclear-active component of a shower with a specified number of particles it is therefore necessary to take into account the contribution of particles with energies $E \sim 10^{12} - 10^{13}$ ev, which appear in the shower at an average frequency of $\sim 10^{-2}$.

In conclusion, let us estimate the energy carried in a shower by nuclear-active particles that appear at a frequency $\lesssim 1$. For this purpose we extend the spectrum of the nuclear-active particles towards the low-energy region assuming that the integral energy spectrum of such particles has a slope not less than that corresponding* to E^{-1}. For a medium shower with $N \sim 10^3 - 10^4$ particles this gives 40% of the energy carried by the electron-photon component. The value obtained for the energy carried by the nuclear-active component indicates that the latter has a substantial role in the development of showers with $N \sim 10^3 - 10^4$ particles. The estimate given in reference 21 for the energy of the nuclear-active component in the limiting case — equilibrium between the electron-photon and nuclear-active components — allows us to state that for an average shower with $N \sim 10^3 - 10^4$ particles this condition is formally satisfied.

CONCLUSIONS

1. The exponent of the energy spectrum of nuclear-active particles at sea level, in the energy range from 10^{12} to 4×10^{13} ev, remains constant at $\gamma = -1.5 \pm 0.2$ in the $10^{12} - 5 \times 10^{12}$ ev range and $\gamma = -1.5^{+0.3}_{-0.2}$ in the $5 \times 10^{12} - 4 \times 10^{13}$ ev range.

2. The coefficient of absorption of nuclear-active particles with energy $\sim 10^{13}$ ev in the atmosphere corresponds to a range of (120 ± 5.5) g/cm^2.

3. The cross section for the interaction between air nuclei and nuclear-active particles remains constant up to $E = 5 \times 10^{12}$ ev; at any rate, it does not drop until $E \geq 10^{13}$ ev.

4. The presence of a broad range of intensities

of air accompaniment for particles with $E \geq 10^{12}$ ev is explained by the different number of interactions between the nuclear-active particles in the atmosphere under unchanged characteristics of the elementary act.

5. Nuclear-active particles of high energy play a substantial role in the development of low-density showers with a total number of particles $N \sim 10^3 - 10^4$. In the development of individual showers of low intensity, one observes large fluctuations in the distribution of energy between the nuclear-active and electron-photon components.

The authors express their gratitude to S. N. Vernov for great help rendered in this work.

---

*Actually, in showers with $N \geq 10^4$ the energy spectrum of the nuclear-active particles, in the frequency region ~1, is characterized by $\gamma \approx -1.1$. The energy spectra in showers with different N can be expected to be similar when expressed in units of E/E_0.

[1] H. Carmichael and F. Steljis, Phys. Rev. 99, 1542 (1955). H. Carmichael, Phys. Rev. 107, 1401 (1957).

[2] K. Greisen, Progress in Cosmic Ray Physics 3, Amsterdam, 1956.

[3] Veksler, Kurnosova, and Lyubimov, JETP 17, 1026 (1947). Azimov, Dobrotin, Lyubimov, and Rozhkova, Izv. Akad. Nauk SSSR, Ser. Fiz. 17, 80 (1953).

[4] Grigorov, Murzin, and Rapoport, JETP 34, 506 (1958), Soviet Phys. JETP 7, 348 (1958).

[5] Anishchenko, Zatsepin, Rozental', and Sarycheva, JETP 22, No. 2, 1952.

[6] Grigorov, Shestoperov, Sobinyakov, and Podgurskaya, JETP 33, 1099 (1957), Soviet Phys. JETP 6, 856 (1958).

[7] L. A. Farrow, Phys. Rev. 107, 1987 (1957).

[8] I. M. Bekkerman, V. A. Dmitriev, et al., Приборы и техника эксперимента (Instrum. and Meas. Engg.) No. 4, 31 (1958).

[9] Dmitriev, Kulikov, and Khristiansen, Paper delivered at Conference on Cosmic Rays, Varenna, 1957.

[10] Abrosimov, Dmitriev, Kulikov, Massal'skiĭ, Solov'ev, and Khristiansen, JETP 36, 751 (1959), Soviet Phys. JETP 9, 528 (1959).

[11] V. A. Dmitriev, J. Tech. Phys. (U.S.S.R.) 27, 205 (1957), Soviet Phys.-Tech. Phys. 2, 179 (1957).

[12] K. Greisen, Phys. Rev. 73, 521 (1948).

[13] E. George, Cosmic Ray Physics, vol. 1, 1954.

[14] Zatsepin, Krugovykh, Murzina, and Nikol'skiĭ, JETP 34, 298 (1958), Soviet Phys. JETP 7, 207 (1958).

[15] Azimov, Dobrotin, et al., Izv. Akad. Nauk SSSR, Ser. Fiz. 17, 80 (1953).

[16] I. P. Ivanenko, Dokl. Akad. Nauk SSSR 107, 819 (1956), Soviet Phys.—Doklady 1, 231 (1956).

[17] G. T. Zatsepin, Dissertation, Phys. Inst. Acad. Sci., 1953.

[18] L. Elliott, Paper delivered at Conference on Cosmic Rays, Oxford, 1954.

[19] G. Cocconi, Nuovo cimento, VIII, Suppl. No. 2, 1958.

[20] Vernov, Gorchakov, Ivanenko, and Khristiansen, JETP 36, 1233 (1959), Soviet Phys. JETP 9, 877 (1959).

[21] Abrosimov, Goryunov, Dmitriev, Solov'eva, Khrenov, and Khristiansen, JETP 34, 1077 (1958), Soviet Phys. JETP 7, 746 (1959).

Translated by J. G. Adashko
181